A Coupled Multiscale Model of Texture Evolution and Plastic Anisotropy

J. Gawad[*,†], A. Van Bael[**,‡], S. K. Yerra[**], G. Samaey[*], P. Van Houtte[**] and D. Roose[*]

[*]*Department of Computer Science, Katholieke Universiteit Leuven, Belgium*
[†]*University of Science and Technology AGH, Poland*
[**]*Department of Metallurgy and Materials Engineering, Katholieke Universiteit Leuven, Belgium*
[‡]*Limburg Catholic University College (KHLim), Belgium*

Abstract. In this paper we present a multiscale model of a plastic deformation process in which the anisotropy of plastic properties is related to the evolution of the crystallographic texture. The model spans several length scales from the macroscopic deformation of the workpiece to the microscale interactions between individual grains in a polycrystalline material. The macroscopic behaviour of the material is described by means of a Finite Element (FE) model. Plastic anisotropy is taken into account in a constitutive law, based on the concept of a plastic potential in strain rate space. The coefficients of a sixth-order Facet equation are determined using the Taylor theory, provided that the current crystallographic texture at a given FE integration point is known. Texture evolution in the FE integration points is predicted by an ALAMEL micromechanical model. Mutual interactions between coarse and fine scale are inherent in the physics of the deformation process. These dependencies are taken into account by full bidirectional coupling in the model. Therefore, the plastic deformation influences the crystallographic texture and the evolution of the texture induces anisotropy of the macroscopic deformation. The presented approach enables an adaptive texture and yield surface update scheme with respect to the local plastic deformation in the FE integration points. Additionally, the computational cost related to the updates of the constitutive law is reduced by application of parallel computing techniques. Suitability of on-demand computing for this computational problem is discussed. The parallelisation strategy addresses both distributed memory and shared memory architectures. The cup drawing process has been simulated using the multiscale model outlined above. The discussion of results includes the analysis of the planar anisotropy in the cup and the influence of complex deformation path on texture development. Evolution of texture at selected material points is assessed as well.

Keywords: multiscale modelling, texture evolution, multilevel model, sheet forming, finite element
PACS: 02.70.-c, 46.15.-x, 46.90.+s, 62.20.F-, 81.40.Lm

INTRODUCTION

The crystallographic texture has a significant influence on the mechanical and physical properties of sheet products as it causes plastic anisotropy. Obviously, this should be taken into account during the simulation of sheet forming processes with the Finite Element (FE) method. The evolution of the texture occurring in the deformed material should be reproduced in the plastic anisotropy of the material. An appropriate and reliable constitutive model for the material should involve the updating of the constitutive law and must correspond to the quantitatively accurate prediction of the texture. This is a challenging task, since phenomena at multiple scales are involved in the physics of the process. These requirements make the entire task complex and computationally costly. Moreover, one has to decide whether the evolution of material properties in the FE simulation should either occur continuously (i.e. in every time step) or whether it can be deferred to selected update temporal points.

The current paper exploits several concepts proposed previously by Van Houtte and co-workers. For the sake of clarity, some of the ideas are briefly recapitulated in the paper. For a detailed description, the reader is referred to the original papers: the Facet method is comprehensively discussed in [1] and the Advanced LAMEL (ALAMEL) model is presented in [2].

MULTISCALE MODEL

The macro-scale part of the model presented in this paper follows the idea of the Finite Element method with an analytical macroscopic yield locus. There are many successful examples in the literature that an accurate analytical expression can describe the plastic anisotropy of the polycrystalline. Such yield locus model can be identified by evaluating a micro-scale model, e.g. one based on the Full Constraint (FC) Taylor assumption [3], a self-consistent model (e.g. [4]) or a more advanced one, such as the ALAMEL model used in this paper. Thus, a strong connection between microscopic phenomena and macroscopic material response is introduced. This link persists even if the microscale properties of the material are assumed to remain constant. However, such formulation does not permit a reliable description at the crystal level. Another, completely different approach discards entirely the analytical yield locus expression and makes use of the Representative Volume Element (RVE) formulation, owing to the homogenisation theory.

We take the aforementioned issues into account in a new multiscale model of a deformation process presented in the paper. In this model, the phenomena occurring at the multiple length scales are mutually dependent. The anisotropy of plastic deformation contingents upon the evolution of crystallographic texture and *vice versa*. The FE mechanical model of cup drawing process is considered as a macroscopic description of the deformed workpiece. The analytical constitutive law describing the plastic anisotropy, based on the concept of a plastic potential in strain rate space, is implemented into the commercial FE code ABAQUS/Explicit.

The plastic anisotropy of textured polycrystalline material can be described by means of a plastic potential in strain rate space. Recently, Van Houtte et al. [1] proposed the Facet method that utilises a homogeneous polynomial to describe the plastic potential. For materials without strain rate sensitivity, the deviatoric stress tensor $\mathbf{S}$ derived from the plastic flow stress can be calculated for a given strain rate tensor $\mathbf{d}$ as:

$$\mathbf{S} = \frac{\partial \psi(\mathbf{d})}{\partial \mathbf{d}}, \tag{1}$$

In the Facet method, the plastic potential $\psi(\mathbf{d})$ in the strain rate space is expressed using the function:

$$\psi(\mathbf{D}) = [G_n(\mathbf{D})]^{\frac{1}{n}}, \tag{2}$$

where $G_n(\mathbf{D})$ is a homogeneous polynomial of degree n and n is an even natural number greater than 1. The Facet method exploits the property of the strain rate tensor $\mathbf{d}$ that it can be converted into a vector $\mathbf{D}$ in a five-dimensional space. Consequently, the Facet equation is given by:

$$G_n(\mathbf{D}) = \sum_{\kappa=1}^{K} \lambda_\kappa \left(S_{\kappa,p} D_p\right)^n, \tag{3}$$

where $\mathbf{D}$ is a five-dimensional strain rate vector, $D_p, p = 1\ldots5$ are the components of the strain rate vector, λ_κ and the components of 5D deviatoric stress vectors $S_{\kappa,p}, p = 1\ldots5, \kappa = 1\ldots K$ are parameters. Einstein summation convention is used for the index p. Provided that $\lambda_\kappa \geq 0$ for all κ and n is a positive even number, it can be proven that the equipotential surface as defined by Equation (2) and Equation (3) is always convex [1].

The identification of the parameters in Equation (3) requires numerous evaluations of the stress vectors for the corresponding nearly equidistant strain rate modes. This can be done by means of the FC Taylor or a more advanced micromechanical model. Previous experience [1] shows that an acceptable approximation of the equipotential yield surface requires a degree $n \geq 6$ and at least 402 strain modes. The amount of strain modes evaluations can be reduced by a factor of two if the stress differential effect need not be accounted for.

For the purpose of the parameter identification, it is suitable to rephrase the Equation (3) in matrix form. The parameters λ_κ can be determined by solving the following system of equations:

$$[W]\{\lambda\} \cong \{C\}, \tag{4}$$

where the vector C selects the equipotential surface and the components of the matrix $W_{ij} = (\mathbf{D}_i \cdot \mathbf{S}_j)^n$ are identified as the homogeneous n-th degree polynomials of the plastic work dissipated per unit volume in function of the macroscopic plastic strain rate $\mathbf{D}$. The 5D deviatoric stress vectors $\mathbf{S}_j$ correspond with the $\mathbf{D}_j$ strain modes for which the micromechanical model calculates the plastic work. The system (4) is solved using the Non-Negative Least Squares (NNLS) algorithm [5], which ensures that all components of λ are positive or zero.

Algorithm 1 The pseudo-code of the texture updating algorithm implemented in ABAQUS user subroutine

Require: **D** is calculated for every integration point
 1: **for all** integration points **do**
 2:     $\mathbf{P} \leftarrow \mathbf{P} + \mathbf{D}dt$
 3:     **if** criterion for updating is satisfied **then**
 4:         Subject the texture to deformation **P**   ▷ run the ALAMEL
 5:         $\mathbf{P} \leftarrow 0$
 6:         **for all** strain modes **do**
 7:             calculate stress tensor **S**   ▷ run the FC Taylor model
 8:         **end for**
 9:         Store the checkpoint data
10:         Calculate λ coefficients by solving system (4)   ▷ identify the Facet model
11:         Commit the updated constitutive law
12:     **end if**
13: **end for**

Texture evolution in the FE integration points is predicted by the ALAMEL micromechanical model [2]. The ALAMEL belongs to the class of statistical models for the plastic deformation of polycrystalline materials. The model follows the Taylor assumption that plastic deformation must be homogeneous for thin regions situated at both sides of the grain boundary. However, one of the advantages of the ALAMEL over the classic FC Taylor approach is related to the stress equilibrium conditions imposed at the grain boundaries in the simulated microstructure. It was shown in [2] that the qualitative predictions of the texture are more accurate than those obtained using the FC Taylor model. The ALAMEL represents the state of the crystallographic texture by means of a discrete form of the orientation distribution function (ODF). The crystallographic orientations are expressed using three Euler angles in Bunge notation [6]. Triclinic class of sample symmetry must be imposed to the original ODF because the initial orthorhombic symmetry is expected to disappear due to the texture updating.

In this work, we assume that the texture may evolve independently in every FE integration point. This evolution is split into intervals between the updating events. An overview of the updating method is presented in Algorithm 1. In order to decide whether such event has to be activated, the history of deformation is being tracked. The state of the material is described by means of the accumulated plastic strain:

$$\mathbf{P}_i = \int_{t_{i-1}}^{t_i} \mathbf{D}dt, \tag{5}$$

where i is the ordinal number of the updating event, **D** is the plastic strain rate as calculated by the FE in the integration point, t_{i-1} is the time of the previous updating event. The time intervals $|t_i - t_{i-1}|$ can be imposed either explicitly or determined on-line using a more elaborated criterion. In this work we utilise the following predicate function to determine whether the texture-related material properties should be updated:

$$f(\mathbf{P}_i) = \left\{ \begin{array}{lll} 1 & : & ||\mathbf{P}_i|| \geq P_{cr} \\ 0 & : & \text{otherwise} \end{array} \right., \tag{6}$$

where P_{cr} is a parameter. The criterion is defined as satisfied if the predicate (6) results in value 1. The activation of the criterion (6) is considered as a necessary condition for modification of the local texture representation. The accumulated plastic deformation $\mathbf{P}_i$ is passed to the ALAMEL model, which applies the appropriate lattice rotations to the crystals belonging to the virtual microstructure. Afterwards, the updated texture data are used as an input for the reconstruction of the plastic potential (2). This step requires series of stress tensor calculations for the prescribed strain modes. The Taylor theory was used [3], assuming the identical critical resolved shear stresses on 24 {110}+{112}<111> slip systems. Provided that the stress components are evaluated, the system (4) is solved. As a result, the updated yield surface is affected by the modification introduced by the texture prediction model.

It is worth noting that the mechanical properties of the material remain constant between the successive updates. However, the time steps used by the FE are very short, which is intrinsic to the explicit time integration solvers.

Computational issues

Keeping in mind that the complexity of the problem translates into the time demanded for computations, we analysed the predominant components of the execution time for our model. For a reasonable value of the parameter P_{cr} chosen as 0.1, the number of updating steps N_u was appraised approximately as $N_u \approx 6000$. This reckoning was made by counting the virtual activations of the criterion (6) observed in the FE simulation of the cup drawing process performed for the constant material properties. If the computer program implementing our multiscale model is executed on a single CPU, the estimation of the time necessary for the computations is given by: $T_s = N_u T_u + T_{FE} = 6000 \cdot 10[\text{min}] + 1620[\text{min}] \approx 43[\text{days}]$, where T_u is the amount of time for a single texture and constitutive model update, T_{FE} is the time spent on the FE calculations.

Algorithm 1 exhibits several opportunities for parallelisation. The iterations of the top-level loop (line 1 in Algorithm 1) can be executed independently of each other. In the current study the workload related to that loop is distributed among the compute nodes of the high performance cluster (HPC) facility. Our implementation takes into account a varying problem size, since the number of updating criterion activations may vary from one time step to another. Instead of requesting a constant pool of the CPUs from the HPC queuing system, the code starts the worker programs on demand, with respect to the task size and the current availability of the idle CPUs in the cluster. Therefore, the actual number of processors that are put at our disposal may vary from several to hundreds. For this reason it is difficult to estimate the speedup of the parallel algorithm in terms of the classic definition. Nevertheless, the assessment of the overall efficiency can be done *a posteriori*.

One can notice that the evaluation of the micromechanical model for the set of strain modes (line 6 in Algorithm 1) can be performed without any communication between the processors. The multicast communication is required only prior to the loop 6, because every processor involved in the task must have the current texture available. The scheme outlined above is suitable for parallelisation on either multi-core (Symmetrical Multi-Processor, SMP) or distributed memory architecture. In the current implementation the former choice is made. Thus, the execution of the loop 1 in distributed among the nodes of the cluster, and the internal loop 6 is parallelised on the multi-processor nodes.

In view of the fact that the two-level parallelisation is implemented in the code, it is possible to tune Algorithm 1 for execution in the HPC environment. For instance, the criterion for texture updating may include an additional part which depends on the global FE time increment number. In order to improve concurrency of the block 3–12 in Algorithm 1, one can decide that the criterion is fulfilled only in the time increments that are multiple of N, where N is a parameter of the algorithm. The distributed checkpointing operation (line 9 in Algorithm 1) allocates the I/O operations over the parallel filesystems. Step 6 in Algorithm 1 can benefit from availability of modern multi-core CPUs, as it shows nearly linear speedup. The aforementioned improvements are utilised to improve the performance of the model.

RESULTS

In this work the cup drawing is considered, which is a simple and typical example of sheet forming process. The investigated material is a low carbon DC01 steel. The model outlined in the previous section has been implemented in the FE code Abaqus/Explicit. The sample is discretised using the reduced integration elements C3D8R. A local coordinate system is attached to every element in the FE mesh. Initially, the coordinate system is common for the entire FE mesh, but the local coordinate systems co-rotate with the material during the simulation. Coulomb friction with the coefficient $\mu = 0.05$ is imposed at the contact surfaces. The Young modulus is assumed 210 GPa and Poisson ratio 0.3. A Swift-type hardening law is used, with the following values of coefficients: $K = 659$ MPa, $n = 0.399$ and $\varepsilon_0 = 2.96 \cdot 10^{-2}$. The coefficients were corrected following the method given in [7]. The Facet expression of degree 6 was used, the parameters of the Equation (3) were determined using 201 strain modes.

The geometry of a calculated intermediate cup is presented in Fig. 1. It can be seen that part of the elements have undergone at least one updating of the material properties. The updates take place in the zones that correspond to the localization of the largest accumulated plastic strain. Forasmuch as the element-by-element updating approach is used, the amount of constitutive law updates is moderate at the early stages of deformation, as is demonstrated in Fig. 1. The final geometry of the cup is shown in Fig. 2. It can be seen in that figure that two ears appear for $0°$ and $90°$ to the rolling direction (RD).

The calculations were performed on the HPC cluster. The parallel machine consists of 256 nodes, which are mainly dual-core and quad-core AMD Opteron systems. The design of our code exploits the fact that the PBS/Maui job system promotes relatively short, parallel jobs. The simulation of the process required 136034 FE time increments to reach the total simulation time $5 \cdot 10^{-3}$s. The actual number of the texture and yield surface updates as counted during the
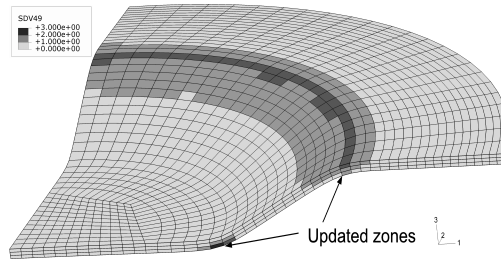
FIGURE 1. The partially deformed sheet during the cup drawing. The finite elements where the update of material properties has occurred are marked gray. Grayscale denotes the number of the updating events in the element. The update of texture and constitutive law is limited to the zones corresponding to the largest accumulated plastic strain
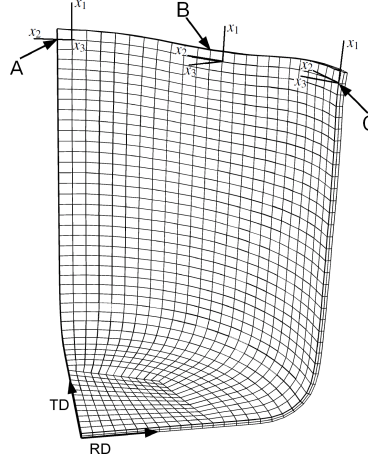

FIGURE 2. The final cup geometry obtained from the multiscale model. The points A, B and C denote the locations of texture measurements. The local reference frames for the experimental textures are indicated with x_1, x_2 and x_3 axes

calculation was $N_u = 5939$. Measured execution time of parallel computations was only $T_p = 2265[\text{min}] \approx 1.57[\text{days}]$. This lead to *a posteriori* estimation of the speedup, $S = \frac{T_s}{T_p} \approx 27$.

In order to verify the results of the numerical model, an experimental study was additionally performed. The analysis included the initial and final state of the material. The measurements of the texture in a cold-rolled DC01 steel sheet (thickness 0.5mm) provided an orientation distribution function (ODF) which was utilized as the initial input data. The texture in the analysed sheet exhibits a strong γ-fibre, the maximal ODF value was 19.04, texture index was 7.108. The discretisation of the ODF consists of 5000 equally-weighted grains. Such a discretisation is considered as sufficiently representative for the lattice orientations in low carbon steel grades [1].

The X-ray measurements of the final texture were taken from the fully deformed experimental cup. The locations of the sampling points are indicated in Fig. 2. The points A, B and C are selected to be placed close to the cup rim at $90°$, $45°$ and $0°$ to the rolling direction, respectively.

The evolution of texture in the point A is shown in Fig. 3. In order to facilitate the evaluation of the results, all the calculated textures are rotated to the coordinate systems used in the experiment. Therefore, in all cases the radial direction of the cup is aligned with the vertical x_1 axis of the experimental sample. To illustrate the evolution of the texture, the sections of ODFs are presented with the ϕ_1 Euler angle ranging from 0 to $360°$ and $\phi_2 = 45°$. According to the update criterion (6), the plastic strain increments of uniform norm $||\mathbf{P}_i|| = P_{cr}$ are applied, $P_{cr} = 0.1$. Figure 3a shows the state of the initial texture, while Fig. 3b presents the state of the texture after deformation $\mathbf{P}_1$, Fig. 3c presents the deformation texture after the second update with deformation $\mathbf{P}_2$ and so on. The $\phi_2 = 45°$ section of the ODF determined for the experimental cup in the point A is presented in Fig. 3j. The texture indices are also listed. The strongly decreased texture index corresponds to the broadening of the original texture. The index increases continuously after all subsequent updates due to increased intensities for particular orientations along the original γ-fibre. A remarkable congruence between the experimental and the ALAMEL-predicted texture can be noticed in that

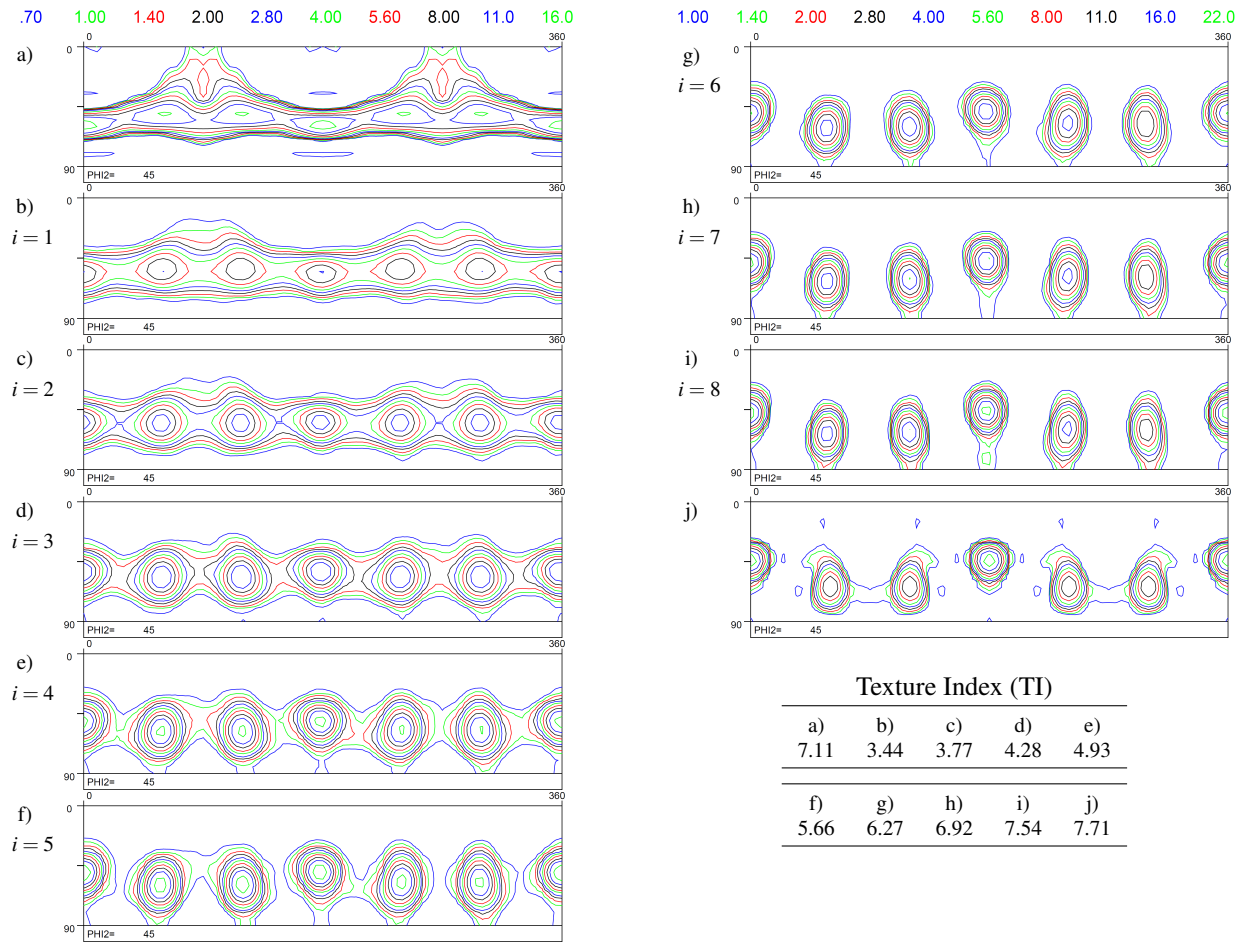**FIGURE 3.** $\phi_2 = 45°$ sections of the ODF for: a) initial experimental texture, b) – i) evolution of the texture in the point A (90° to RD) predicted by the ALAMEL model for the successive deformations $\mathbf{P}_i$ ($||\mathbf{P}_i|| = 0.1$), j) – texture measured in the corresponding point of the experimental cup. Texture index is given for every texture a) – j)

figure. This is particularly relevant for the final deformation texture, see Figures 3 i and 3 j. When comparing the main texture component, one has to remark that the intensity of the texture is very similar in both cases. Additionally, this is confirmed by the texture index of the experimental texture which coincides with the ALAMEL result. It shows a substantial improvement to the previous findings (e.g. [8, 9]), where the angular position of the texture components was correctly identified by means of FC Taylor model, but the intensity of the texture was overestimated.

The agreement between the yield locus calculated from the measured textures and the simulated one can be visually inspected using a π-plane section of stress or strain rate space. The following relations are satisfied for the π-plane: $d_{11} + d_{22} + d_{33} = 0$ and $S_{11} + S_{22} + S_{33} = 0$ for strain rate and stress space, respectively. Figure 4 shows the π-plane sections of yield locus in stress space and equipotential surface in stain rate space, calculated for the point A. As seen in that figure, the shape of the equipotential surface calculated using the Taylor model on the basis of the texture evolution predicted with the ALAMEL is fairly consistent with the result obtained for the real deformation texture. The convexity of the yield surface is also reproduced by the model.

Successive deformation of the material leads to a new deformation texture, as it can be seen in Fig. 5. The $\phi_2 = 45°$ sections of the ODF for point B reveal only small discrepancy between prediction and measurement. The final texture in point B is approximately orthorhombic and strongly resembles the final texture in point C. The texture in point A is nearly identical to the one in point C. It is noticeable that the texture indices of the predicted ODF in the three points significantly correspond to the experimental ones.

The plastic anisotropy of the flat samples is commonly characterised by the q-values, i.e. the ratio of the plastic strain
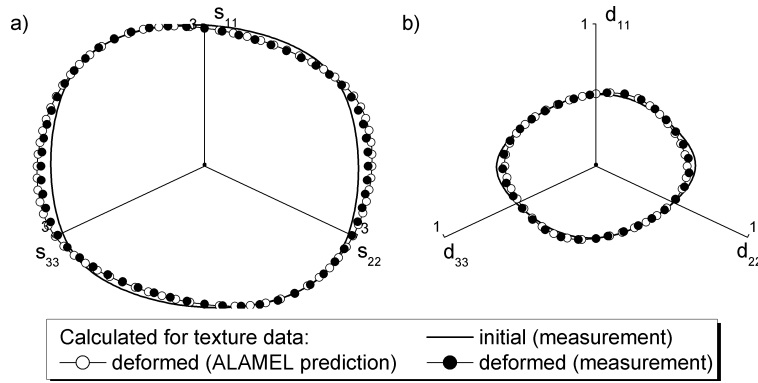
FIGURE 4. π-plane section of a) yield locus in stress space and b) equipotential surface in stain rate space. The sections are calculated for the texture data in point A, as denoted in Fig. 2: plain line – initial texture, open symbols – final texture prediction shown in Fig. 3h, filled symbols – experimentally determined deformation texture shown in Fig. 3i
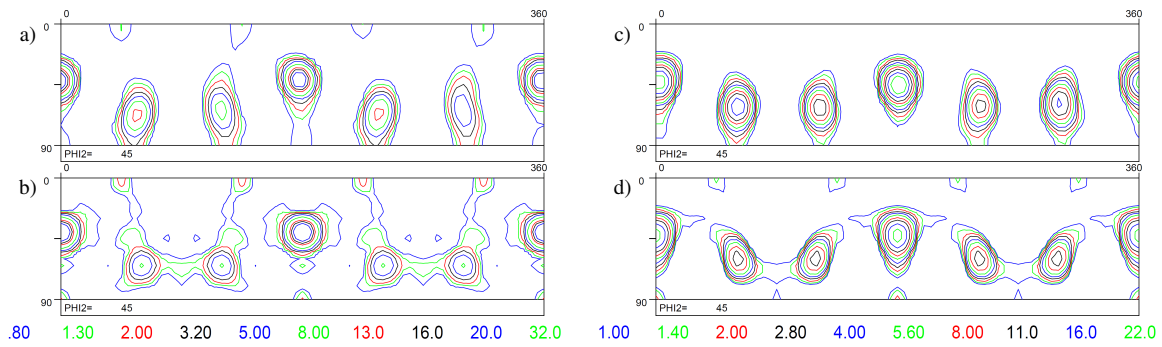

FIGURE 5. Comparison of the final deformation texture: a), c) are predicted by the ALAMEL in point B (45° to RD) and C (0° to RD), respectively, b), d) were determined experimentally in the corresponding points. Texture index: a) TI=8.363, b) TI=8.265, c) TI=7.541, d) TI=7.443

in the width direction to the one in the longitudinal direction. The relation between Lankford r-value and q-value is expressed by $q = r/(r+1)$. The subsequent changes of the crystallographic texture induce the accommodation of plastic anisotropy as shown in Fig. 6. For better comparison with results calculated for the experimental texture, the q-values are presented as a function of the angle to the sample radial direction, i.e. in the experimental sample reference frame. The filled symbols in Fig. 6 denote the results obtained for the experimental textures following the method described in [10]. A smooth evolution of the planar anisotropy towards a new stable configuration is observed.
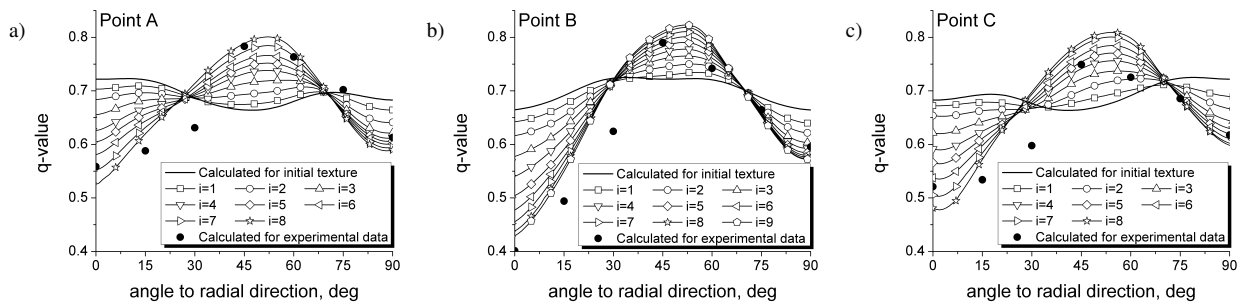

FIGURE 6. Evolution of q-values in consecutive update steps (open symbols). The initial q-values are denoted with plain line, filled symbols denote q-values calculated for the final texture measured on the experimental cup. In the plot for the point A the lines are calculated using the intermediate textures b) – i) as shown in Fig. 3, respectively. Number of plastic strain increments $\mathbf{P}_i$ of the norm P_{cr} is denoted by the index i

Interestingly, in the point A and C the anisotropy after the first texture update seems to be substantially lower than in the initial material. The subsequent updates lead to an increase of q-value variation which finally ranges from 0.52 to 0.8 in point A and 0.48 to 0.81 in point C, respectively. This is not the case for the points B, where the tendency towards augmented planar anisotropy is instantaneously obtained. The agreement between q-values obtained from the measured textures after deformation and the simulated textures is satisfactory, although some discrepancies are observed for the point C.

CONCLUSIONS

A new multi-scale approach to crystallographic texture prediction in a complicated metal forming process was presented in the paper. The concept of analytical constitutive law describing the plastic anisotropy in the FE was applied in the model. A state-of-the-art Facet method for plastic potential in strain rate space was implemented into the FE code. Owing to the successive reconstructions of the yield locus, coupled to the evolution of the crystallographic texture, the mutual interactions between micro- and macro-scale are taken into account. Therefore, the plastic deformation influences the texture, while the evolution of the texture induces the changes in the anisotropy of macroscopic deformation. The presented approach enables the adaptive texture and yield surface update schema with respect to the local plastic deformation in the FE integration points. Despite the fact that the model does not predict the true continuous evolution of the microstructural and mechanical properties, the quantitative forecast of the micro- and macro-scale material behaviour is reasonably accurate.

The results of this study confirm the capability of the ALAMEL model to predict the evolution of the crystallographic texture in steels. In comparison to the previous attempts (e.g. [8, 9]) in which the FC Taylor theory was used, the quantitative accuracy of texture intensities is improved.

The limitations of the model due to its computational complexity are discussed in the paper. To overcome these restrictions, parallelisation techniques have been implemented in the code. A satisfactory speedup of the computations on a HPC cluster compared to a single processor calculations is achieved.

ACKNOWLEDGMENTS

REFERENCES

1. P. Van Houtte, S. K. Yerra, and A. Van Bael, *International Journal of Plasticity* **25**, 332 – 360 (2009).
2. P. Van Houtte, S. Li, M. Seefeldt, and L. Delannay, *International Journal of Plasticity* **21**, 589 – 624 (2005).
3. G. I. Taylor, *J. Inst. Metals* **62**, 307–324 (1938).
4. A. Molinari, S. Ahzi, and R. Kouddane, *Mechanics of Materials* **26**, 43–62 (1997).
5. C. L. Lawson, and R. J. Hanson, *Solving Least Squares Problems*, Prentice-Hall, 1974.
6. H. Bunge, *Texture Analysis in Materials Science*, Butterworth, London, 1982.
7. S. Li, E. Hoferlin, A. Van Bael, P. Van Houtte, and C. Teodosiu, *International Journal of Plasticity* **19**, 647 – 674 (2003).
8. J. Winters, *Implementation of a texture-based yield locus into an elasto-plastic finite-element code*, Ph.D. thesis, K.U. Leuven (1996).
9. E. Hoferlin, A. Van Bael, and P. Van Houtte, "Influence of texture evolution on finite-element simulation of forming processes," in *Proc. of 12th International Conference on Textures and Materials*, 1999.
10. H. Bunge, *Kristall und Technik* **5**, 145–175 (1970).